

**TITLE PAGE:**

Impact of particulate deproteinized bovine bone mineral and porous titanium granules on early stability and osseointegration of dental implants with narrow marginal circumferential bone defects

Anders Verket, DDS, PhD\*, Ståle Petter Lyngstadaas, DDS, B Eng, PhD#, Hanna Tiainen, MSc, PhD#, Hans Jacob Rønold, DDS, PhD§, and Johan Caspar Wohlfahrt DDS, MS, PhD\*

\* Department of Periodontology, Institute of Clinical Dentistry, University of Oslo

# Department of Biomaterials, Institute of Clinical Dentistry, University of Oslo

§ Department of Periodontology, Institute of Clinical Dentistry, University of Oslo

Corresponding author:

Anders Verket, Department of Periodontology, Institute of Clinical Dentistry, P.O. Box 1109 Blindern, NO-0317 OSLO, Norway, Email: [anderver@odont.uio.no](mailto:anderver@odont.uio.no), Phone: +47-22852064

**Running head title** particulate graft peri-implant bone defect

**Key words** dental implants, biomaterials, experimental study, bone regeneration

## **ABSTRACT:**

The use of two particulate bone graft substitute materials in experimental narrow marginal peri-implant bone defects was investigated, with respect to early bone healing and stability of implants. Porous titanium granules, oxidized white porous titanium granules and demineralized bovine bone mineral were characterized *in vitro*, after which the two latter materials were tested in experimental peri-implant bone defects in six minipigs, with empty defects as control. After mandibular premolar extraction, the top 5 mm of the alveoli were widened to 6 mm in diameter, followed by placement of 6 implants, 3 on each side, in each pig. Six weeks healing was allowed.

The white porous titanium granules had the better mechanical properties. No significant differences were found in resonance frequency analysis directly after compacting or healing, and similar quantities of defect bone formation were observed in microcomputed tomography for all groups. Histomorphometric analysis demonstrated a more coronal "bone-to-implant contact" in the demineralized bovine bone mineral group, which also displayed more defect bone fill as compared to the white porous titanium granule group.

The better mechanical properties observed for the white porous titanium granules seemed of negligible relevance for the early stability and osseointegration of implants.

## **MANUSCRIPT:**

# **Impact of particulate deproteinized bovine bone mineral and porous titanium granules on early stability and osseointegration of dental implants with narrow marginal circumferential bone defects**

## **Introduction**

Fresh extraction sockets frequently present dimensions greater than the implant diameter, and immediate implant placement may therefore result in a gap between the implant surface and the marginal alveolar ridge. This is often referred to as the “jumping distance”, which may also be encountered in staged implantation procedures<sup>1</sup>. A review has recommended grafting for a jumping distance of > 2 mm, but further disclosed that there is a current controversy as to how big the gap should be (1-2 mm or wider) for potential benefit from bone graft substitute materials<sup>2</sup>. Also, there is no consensus on which bone graft substitute material is most suitable for regeneration of bone and for dental implant support in marginal peri-implant bone defects<sup>1,3</sup>. Bone graft substitute materials for this indication should preferably enhance early stability and proliferate osseous support for the implants.<sup>4</sup>

White porous titanium granules (WPTG), a synthetic bone graft substitute material, may be a candidate material. WPTG is derived from heat treatment and oxidation of porous titanium granules (PTG) and the process alters its physical characteristics and colour, which according to the manufacturer is intended for use in aesthetically sensitive areas. Contrary to WPTG, PTG have been characterized previously<sup>5</sup>. However, previous experimental studies have demonstrated an osteoconductive potential of the WPTG<sup>6,7</sup>. In the *in vivo* part of the present study, WPTG

was preferred due to the risk of plastic deformation of the metallic PTG during application and potential implant load in the experimental model<sup>5</sup>. Deproteinized bovine bone mineral (DBBM) is a naturally derived bone graft substitute material and one of the most studied and used materials in conjunction with implant dentistry. Several studies have been performed previously with a design similar to the present study, and application of DBBM was not found to be advantageous for the implant osseointegration in gaps up to 1.25 mm for, although a benefit was suggested for gaps exceeding 2 mm<sup>8-10</sup>. WPTG has not been evaluated in such a model and also the impact of bone graft substitute materials on early implant stability and osseointegration before 8 weeks has not been extensively researched previously.

The present study was conducted to characterize and evaluate the effect of two particulate bone graft substitute materials with hypothesized different mechanical properties applied in experimental marginal peri-implant bone defects, with respect to early bone healing and stability of implants. DBBM and WPTG were compared *in vivo*, and porous titanium granules (PTG) were included in the *in vitro* analysis for comparison. The hypothesis was that the stronger bone graft material provided better primary implant stability and thus enhanced early bone healing and osseointegration *in vivo*.

## **Materials and Methods**

To visualize and analyse the pore structure, a scanning electron microscope (SEM; TM-1000, Hitachi High-Technologies, Tokyo, Japan) and a commercially available microcomputed tomography (microCT) desktop scanner (SkyScan 1172, Skyscan N.V., Kontich, Belgium), were used. A fixed volume (0.5 ml) of the bone graft substitute material was placed in an eppendorf tube and scanned at 8  $\mu\text{m}$  voxel resolution using

100 kV and 100  $\mu$ A source voltage and current with standard Al + Cu filter. Pore structural characteristics were assessed as previously described<sup>5</sup> in the middle of each scanned sample within a volume of interest (VOI) measuring 3 mm in height and 8 mm in diameter. For SEM imaging, the bone graft substitute materials were viewed with backscattered electrons at 15 kV acceleration voltage. Compressive mechanical testing (Zwicki, Zwick/Roell, Ulm, Germany) was conducted as previously described<sup>5</sup> to evaluate the mechanical strength of the different bone graft substitute materials. Briefly, confined column of 300  $\mu$ L granules of each material was loaded at a rate of 2.5 mm/min until a fixed load of 850 N was reached (n = 3). Compressive strength was estimated from the load-displacement curves as theoretical load corresponding to the transition from the initial linear region, where the sample retains its porosity to the linear compaction region, where porosity is eliminated. Compact volume was calculated as the reduction in volume due to elimination of porosity.

The animal experimental study was performed in six female minipigs (Göttingen minipig<sup>TM</sup>, Sus Scrofa, Ellegaard A/S, Dalmose, Denmark) aged 17 to 19 months and weighing 38 to 44 kg. The animals were acclimatized in the local facilities (University Hospital Malmö, UMAS, Malmö, Sweden). Preparation of animals as well as animal management and care followed routine protocols approved by the institutional review board of UMAS. Ethical approval for the experiment had been obtained from the institutional review board at UMAS animal experiment ethical committee Malmö-Lund M130-06. The animals were maintained under general anaesthesia using ketamine hydrochloride 50 mg/ml (Ketalar, Pfizer AB, Sollentuna, Sweden), and midazolam 5 mg/ml (Dormicum<sup>®</sup>, Roche, Basel, Switzerland). After visual inspection of the animals, the pigs were shaved around the mouth and the skin was rinsed with chlorhexidin 5 mg/ml in 60% ethanol (Apoteksbolaget, Stockholm, Sweden). Infiltration anaesthesia, 3.6

ml lidocaine 10 mg/ml and adrenalin 5 µg/ml (Xylocaine®, Astra Zeneca, Södertelje, Sweden) was placed in the muco-buccal fold, where after deposits of plaque and calculus was carefully removed. After a marginal incision from the mandibular first premolar to the first molar, with distal and mesial releasing incisions, a muco-periosteal flap was raised in order to expose the teeth and the alveolar bone to facilitate extractions of the premolar teeth P2, P3 and P4. Premolar teeth P2, P3 and P4 were carefully extracted and the empty alveoli were thoroughly inspected to make sure no root remnants were left in the sockets. The marginal 5 mm of the alveoli were widened into standardized defects of 6 mm in diameter with a twist drill. A total of 36 implants (3.25 X 11.5 mm, Full Osseotite®, MicroMiniplant™, Biomet 3i Nordic AB) were installed into the extraction sites creating a marginal void between the lateral wall of the implant and the alveolar wall of ~1.4 mm (Fig. 1a). The most coronal part of the implant neck was placed flush with the crestal bone. The implant stability quotient (ISQ) was assessed by resonance frequency analysis (RFA) (Osstell™, Osstell AB, Gothenburg, Sweden) at the time of implant installation. The measurement was performed four times in four directions and the average number was calculated and recorded. Randomization was performed on a quadrant level to graft the alveoli with heat oxidized PTG (Tigran™ White, Tigran Technologies AB, Malmö, Sweden) (n=12), (DBBM, Bio-Oss™, Geistlich Pharma, Wolhausen, Switzerland) (n=12), whereas control sites were left unfilled (sham) allowing a blood clot to form in the defect around the implant (n=12). After application of the graft material, implant stability was again assessed by RFA in the two test groups, where after cover screws were inserted. Periosteal releasing incisions were placed for passive flap adaptation and submersion of the implants. The surgical sites were finally closed with resorbable polyglactin sutures (Vicryl® 4.0, Polyglactin 910, Ethicon Inc., Somerville, NJ, USA)(Fig. 1b). Particular attention was made to ensure that

the mucosal flap completely covered the bone defects and that it was passively adapted and stably fixated. The animals were kept on a soft diet for one week after the surgery. Antibiotics, benzylpenicillinprokain 250 mg/ml and dihydrostreptomycinsulfate 200 mg/ml (Streptocillin vet, Boehringer Ingelheim GmbH, Ingelheim, Germany), and analgesic, buprenorfin 3ml, 0.3 mg/ml (Temgesic®, Schering-Plough, Brussels, Belgium), were administered at a dose of 1 ml/10 kg once daily for three days after surgery. Six weeks after implantation the pigs were given a lethal injection of 40 ml pentobarbital sodium (Mebumal, Apoteksbolaget, Stockholm, Sweden), 100 mg/ml in spiritus fortis 290 g / 1000 ml. A soft tissue punch procedure was employed in order to expose the implants and the RFA was performed again. The jaw segments were excised en bloc and submerged in freshly prepared, refrigerated (4 °C), phosphate buffered formalin with a pH of 7.4. The specimens were then dehydrated in an ascending series of alcohol rinses prior to embedding in a light-curing methacrylate based resin (Technovit 7200 VLC, Heraeus Kulzer GmbH, Wehrheim, Germany). The resin embedded mandibular jaw segments were cut with an Exakt® saw (Exakt, Norderstedt, Germany) into smaller parts representing single implant sites. Each implant site was scanned with a microCT (SkyScan 1172, SkyScan N.V.). All scans were obtained at 100 kV and 100 µA. A filter was used to optimize the contrast. The pixel size was set to 6.0 µm. The scan was done at 360° rotation and three frames averaging a rotation step of 0.3°. Reconstruction software (Nrecon V 1.6.1.5., Skyscan N.V.) was used to create 3D images. A ring artifact correction of 16 and beam hardening correction of 40% were used. The 3D images were further analyzed using the CTAn software (CTAn., v.1.8.1.2., SkyScan N.V.). A volume of interest (VOI) was constructed to analyze the percentage of new bone formation (BV%) in the marginal peri-implant defect. A circumferential compartment extending 1.2 mm (200 voxels) perpendicularly from the vertical implant surface in the top 5 mm

measured from the implant shoulder, was analyzed (Fig. 2). If a part of the VOI had been accidentally removed when dividing the entire jaw into smaller segments, the missing volume was not included in the VOI. Similarly, if an adjacent tooth was observed compromising bone formation in a part of the defect, the affected volume was excluded from the VOI in the microCT analysis. The threshold values for titanium and bone were determined by superimposing segmented binarized images over original grayscale images<sup>11</sup>. To prepare the histological sections, bucco-lingual slices containing the central part of each implant were cut. The sections were further ground and polished down to a thickness of approximately 70  $\mu\text{m}$  (Polycut-S, Reichert-Jung, Leica Microsystems, Wetzlar, Switzerland) and stained with hematoxylin and eosin (HE). Histological sections were thus prepared according to the cutting-grinding technique<sup>12,13</sup>. For the histomorphometry, digital images were captured (Olympus DP50, Olympus, Aartselaar, Belgium) using a software (Cell<sup>^</sup>B, Olympus soft imaging solutions GmbH, Münster, Germany). A light microscope was used to obtain the images (Leica DMRBE, Leica Microsystems) under 12.5X magnification. Several images were taken for each implant site and stitched together in Adobe Photoshop CS5 (Adobe Systems, Orem, UT, USA) with the photomerge function. All areal and perimetric measurements were performed using the ImageJ software (ImageJ 1.44o, National Institute of Health (NIH), Bethesda, MD, USA). The linear distance between the shoulder of the implant and the most coronal level of bone to implant contact (FBIC) was determined (Fig. 2). The percentage of bone-to-implant contact (BIC%) was measured both in the defect region and the remaining apical region of the implant (Fig. 2). Only the vertical sides of the implants were measured to determine the BIC%, which was measured on all sections obtained from one implant site and then averaged. The areal percentage of bone and residual bone graft material of the total defect area was determined only in the most central section

with respect to the implant diameter. The bone and the residual bone graft material were distinguished and given different colours using the background eraser tool in the computer software Adobe<sup>®</sup> Photoshop CS5 (Adobe Systems, Orem, UT, USA). The area occupied by bone and/or bone graft substitute material was divided by the total defect area. To confirm new bone formation in the defects, the histological sections were additionally analyzed by energy-dispersive x-ray spectroscopy (EDX) at 15 kV accelerating voltage with backscatter electrons to acquire a qualitative chemical surface characterization and elemental analysis. This was performed with an acquisition time of 50 seconds (SwiftED-TM, Hitachi High-Technologies, Tokyo, Japan) on a tabletop SEM (TM-1000, Hitachi High-Technologies). The sections were placed on a 45° angled stub, and the SEM images were analyzed with the computer software (SwiftED-TM, Hitachi High-Technologies), using a detector resolution of 148 eV.

Comparison across groups were performed using a parametric one-way ANOVA. When the normality test failed, Kruskal-Wallis one-way ANOVA on ranks was performed. All statistical analyses were performed using Sigma Plot 12 (Aspire Software International, Ashburn VA, USA). Statistical significance was set at a 0.05 level.

## **Results**

### *In vitro* material characterisation

The scanning electron microscope images demonstrate the surface and porosity of the PTG, WPTG and DBBM (Fig. 3). A different pattern of porosity was observed in the various materials. Single PTG and WPTG granules demonstrated small pores throughout

every granule, whereas the porosity of single DBBM granules appeared limited. The inter-granular porosity however seemed larger for the irregularly shaped DBBM granules. The impact of the heat treatment can be observed as the overall WPTG granule structure appear smoother, less sharp-cornered and divaricate as compared to the pre-heat-treatment appearance. The surface structure on the other hand, appear rougher and more irregular after heating. Macroscopically, the DBBM granules appear less irregular and smoother than the PTG and WPTG. At higher magnifications the surface structure of the DBBM granules appear rough and irregular, much like the WPTG granules (Fig. 3).

The compressive strength of DBBM was significantly lower as compared to WPTG ( $P=0.043$ ) and PTG ( $P=0.042$ )(Fig. 4). The compact volume was reduced significantly more in the DBBM group as compared to WPTG ( $P=0.009$ ) and PTG ( $P=0.01$ ). The interconnectivity of loosely packed granules followed the same pattern in all groups (Fig. 4), but the DBBM granules were consistently more porous and the WPTG consistently less porous through interconnection sizes of up to 200  $\mu\text{m}$ .

#### *In vivo* findings

Three buccal dehiscences were noted following the tooth extractions. Two of these were in the DBBM group and one in the sham group. For one implant in the WPTG group primary stability was not accomplished after placing the bone graft material in the defect. This implant was excluded from the RFA analysis. At harvest this implant was found immobile and thus included in the study for the remaining analyses. All but one implant were in place after six weeks of healing. The lost implant was in the DBBM group. Also, one implant in the sham group was mobile at the time of harvest. These two implants were excluded from all analyses. Twelve WPTG sites, eleven DBBM and sham

sites were therefore included in the final analyses. Six implant exposures; five in the WPTG group and one in the DBBM group were noted at harvest. Healing was uneventful at the remaining sites.

In the resonance frequency analysis, the mean ISQ value at implantation was 52.0 ( $\pm 7.1$ ), 53.2 ( $\pm 10.9$ ) and 55.3 ( $\pm 7.3$ ) for the WPTG, DBBM and sham groups, respectively. After packing the bone graft substitute in the defect prior to healing, the ISQ value for the WPTG and DBBM groups were 53.2 ( $\pm 7.2$ ) and 52.8 ( $\pm 11.4$ ), respectively, which was non-significant as compared to baseline. At termination the corresponding ISQ values were 67.1 ( $\pm 8.2$ ), 71.5 ( $\pm 9.1$ ) and 70.0 ( $\pm 2.4$ ) for the WPTG, DBBM and sham groups, respectively. All mean ISQ values increased over the healing period but were not statistically significantly different across groups.

In the microCT analysis, the BV% of the VOI was 36.8 ( $\pm 8.8$ ), 36.3 ( $\pm 7.5$ ) and 36.5 ( $\pm 6.4$ ) for the WPTG, DBBM and sham groups, respectively. No statistically significant differences between groups were observed. The percentage of newly formed bone in the VOI ranged from 10.8% to 50.3%. Several implant sites, all groups represented, did not contain the full defect volume due to erroneous saw cutting, and a few sites had tooth structures adjacent to the defect volume. The VOI of these sites were modified in order to exclude the missing volume or the part of the volume compromised by the adjacent tooth structures.

Histologically, new mineralized connective tissue had formed within all former defect compartments. The newly formed mineralized connective tissue was predominantly woven bone. Either DBBM or WPTG particles were observed within the healed defects at all test sites. Particles were embedded in non-mineralized loose vascular connective tissue or contiguous with newly formed bone (Fig. 5a,c,d). WPTG

and DBBM particles were never observed in contact with the implant. In general, new bone formation had resolved parts of the marginal defect, in particular adjacent to the former base and the lateral walls (Fig. 5a,b). Consequently, more bone had formed in contact with the implant at the base of the former defect as compared to the more coronal areas. Graft materials localized close to the lateral walls and the base of the former defect were predominantly embedded in bone, whereas graft materials near the implant surface in the coronal part of the defect were more often observed embedded in non-mineralized loose vascular connective tissue. This observation was made both in the WPTG and DBBM sites. However, a different pattern of bone formation was evident in a limited number of sites. In one single site from each group, pronounced bone formation was observed in the coronal area of the defect, whereas the bone formation at the base of the defect was moderate (Fig. 5e). In both WPTG and DBBM groups, bone graft substitute materials were sometimes observed outside of the defect completely embedded in gingival connective tissue. In the apical non-defect area most implants were integrated in bone. In five sites, a tooth was observed in proximity to the former defect. In two of these sites, the tooth and or the periodontal ligament bordered the area of the defect. Importantly, implant placement in proximity to a tooth and or the periodontal ligament seemed to influence the implant osseointegration. The one side of the implant next to the tooth structure often demonstrated limited osseointegration whereas the opposite side of the implant demonstrated osseointegration similar to that of implants not installed in proximity to teeth. This was observed to various extents in the tooth-involved sites, of which two were in the WPTG group, and one each in the DBBM and the sham groups. The fifth implant site in proximity to a tooth structure was the implant in the sham group excluded due to mobility at the time of harvest. The EDX analysis demonstrated that the newly formed bone contained a similar quantity of

calcium and phosphorous as the old bone adjacent to the former defect. A considerable area of the tissue judged as loose vascular connective tissue demonstrated contents of both calcium and phosphate, although at a lower relative quantity as compared to the old bone. This may suggest presence of immature bone matrix. Other areas of the loose vascular connective tissue did not contain significant amounts of calcium and phosphorous.

In the histomorphometric analysis (Fig. 6), the BIC% in the defect was 13.0 ( $\pm$  10.5), 21.9 ( $\pm$  13.7) and 18.9 ( $\pm$  15.2) for the WPTG, DBBM and sham groups, respectively, and no significant differences between the groups were found. In the apical non-defect region the corresponding BIC% was 62.0 ( $\pm$  20.4), 69.8 ( $\pm$  16.9) and 65.7 ( $\pm$  23.7) (n.s.). The mean mm FBIC was 3.5 ( $\pm$  0.8), 2.0 ( $\pm$  1.4) and 3.3 ( $\pm$  1.2) for the WPTG, DBBM and sham groups, respectively. The FBIC was statistically significantly more coronal in the DBBM group as compared to compared to the WPTG group ( $P=0.009$ ) and the sham group ( $P=0.02$ ). The areal percentage of defect bone fill was 33.0 % ( $\pm$  9.8), 51.7 % ( $\pm$  13.3) and 46.1 % ( $\pm$  17.4) for the WPTG, DBBM and sham groups, respectively. There was significantly more bone fill in the DBBM group compared to the WPTG group ( $P=0.008$ ). The areal percentage of residual graft material was 15.5 % for the WPTG group which was significantly higher ( $P=0.02$ ) compared to the 7.2 % of the DBBM group. When adding together the defect bone fill and the residual graft material within the defect, the total defect fill was 48.6 % ( $\pm$  14.3), 58.9 ( $\pm$  12.9) and 46.1 % ( $\pm$  17.4) for the WPTG, DBBM and sham groups, respectively (n.s.).

## **Discussion**

The WPTG demonstrated a higher compressive strength and was less prone to compact volume reduction as compared to DBBM. However, as compared to the implants in the DBBM and sham groups, the implants in the WPTG group did not demonstrate enhanced early implant stability and osseointegration *in vivo*. Instead, the results indicated enhanced early osseous healing in marginal peri-implant bone defects packed with DBBM.

WPTG and PTG were comparable in terms of mechanical properties, but seemed to differ in the structural and surface properties. To the best of the authors' knowledge, this is the first study comparing WPTG and DBBM in an *in vivo* model. The present study suggests that the compressive strength of WPTG is closer to human mandibular trabecular bone than is DBBM<sup>14</sup>. However, the higher compressive strength and resistance to compact volume reduction observed for the WPTG granules seemed to be of negligible relevance for the early stability and osseointegration of implants when grafted in marginal circumferential bone defects. In a previous *in vitro* study where DBBM was compared to PTG, a higher compressive strength and resistance to compact volume reduction was found for PTG<sup>5</sup>, which is in agreement with the present study. Except for the FBIC analysis, the results of the DBBM group differed marginally from the sham group. This finding is in agreement with previous similar studies in the dog<sup>8,9</sup>. The studies by Botticelli et al. and Polyzois et al. reported on the use of DBBM after 4 months healing time, and neither study found the use of DBBM to improve BIC, FBIC or defect closure in defects with a gap up to 1.25 mm, whereas a benefit was suggested for defect gaps exceeding 2 mm<sup>8,9</sup>. In a similar study by Antunes et al.<sup>10</sup>, marginal circumferential peri-implant bone defects with a gap of 1.25 mm were evaluated after 8 weeks healing. The defects were grafted with either hydroxyapatite/tricalcium phosphate, autogenous

bone, or DBBM, and both RFA and histomorphometric analyses were performed. The authors did not find the use of bone graft substitute materials to be advantageous for the implant stability or defect closure after eight weeks healing. The present study had a shorter healing time of six weeks. The better FBIC outcome in the DBBM group in the present study may be due to the short healing time, as the sham defects are not provided a scaffold to support osseous growth, but rely on bone formation originating from existing osseous walls, which may require more time. Collectively, the experimental studies on healing of marginal circumferential peri-implant bone defects suggest that for a bone graft substitute material to outperform the osteogenic potential of the blood clot in self-contained empty defects of 2 mm or less provided sufficient healing time, and to render improved stability and osseointegration of dental implants, requires exceptional modulation of osteogenesis. In terms of formation of new bone tissue within marginal peri-implant defects with a gap size in this range, it may not even be possible for non- or slowly resorbable materials to compare to the blood clot since these materials inevitably occupy a considerable portion of the defect volume. There is evidence to suggest the implant surface characteristics influence the bone healing in peri-implant defects. Circumferential gaps seem more reluctant to heal around machined implant surfaces<sup>15,16</sup>, whereas a variety of rough implant surfaces seem to enhance the bone healing<sup>1,8,10,17</sup>. In the present study Osseotite implants were used, which also have been used in similar studies previously with comparable results for DBBM and defects left empty<sup>8</sup>. However, care should be exercised in extrapolating the results of this study to similar studies with other implant designs.

A previous study reported that contact between the implant and bone at the neck region of the implant affect the ISQ value considerably as compared to contact in the

apical region<sup>18</sup>. Thus, one may speculate whether packing bone graft substitute materials into marginal peri-implant defects in order to support the implant stability, may affect the ISQ value. However, no such increase in the ISQ value for either test group was observed prior to healing in the present study. The two different bone graft materials with different properties did not seem to influence the immediate implant stability or the implant stability during early healing. These findings may potentially have been different if the materials were packed more tightly, but excessive force may again damage the structure of the bone graft materials.

No differences were observed across groups in the microCT analysis. In fact, the mean BV% in the three groups seemed to coincide, despite a wide range. The similar radiodensity of the WPTG and the implant, and of the DBBM and the new bone, implied certain limitations to the microCT analysis. The WPTG group had a larger mean VOI due to difficulties in segmenting the implant from bordering WPTG. Comparison to the other groups was feasible as the bone volume was measured in relative values, and the larger VOIs were for the most part limited to the former defect compartment. The DBBM could be distinguished from bone visually, but exclusion of DBBM was not possible in the software without simultaneously excluding high-radiodensity bone. Therefore the greyscale-threshold setting applied to detect new bone had to be limited. This limited threshold was applied to all sites in all three groups, and the 'true' quantity of bone in the microCT analysis may therefore be slightly underestimated in all three groups.

The percentage of newly formed bone within the defect in all three groups, assessed by histomorphometry, was less than what was observed in a four month study in the dog<sup>1</sup>. In that study non-grafted peri-implant defects 1.25 mm or 2.25 mm wide and 5 mm deep, demonstrated considerably more defect bone fill compared to the

present study. Furthermore, the authors reported a more coronal level of FBIC and a higher defect BIC%. Again, this points to the early time point for evaluation in the present study. The new bone formation in most sites seemed to originate from the lateral walls and the base of the defect. This has been described as 'distance osteogenesis'<sup>19</sup>, and has been demonstrated in several studies with different healing times<sup>10,20,21</sup>. Related to this observation, the position of the graft substitute material within the defect seemed to determine whether the graft particles were surrounded by new bone or by loose vascular connective tissue, which suggests a passive osteoconductive role of both materials tested in this model.

The benefit of using barrier membranes for bone defects similar to those in the present study is equivocal. Utilization of membranes may result in premature exposure and compromised healing<sup>22</sup>. Botticelli et al. compared peri-implant defects grafted with DBBM to non-grafted defects (1.25 mm wide, 5 mm deep), with and without collagen membranes<sup>9</sup>. The authors reported similar values for BIC% and defect bone fill in all groups, although a more coronal level of FBIC was found in the groups covered with membranes. A recent clinical study reported similar outcomes for regenerative treatment of peri-implantitis lesions comparing the use of DBBM and a collagen membrane to porous titanium granules alone<sup>23</sup>.

The lack of experimental groups with barrier membranes covering the bone defects is a limitation of the present study. The potential of the tested materials for guided bone regeneration could thus not be tested. The principal reason for not using membranes was related to the aim of the study, which was to evaluate the impact of the two particulate bone graft materials. Experimental groups including barrier membranes certainly could have improved and extended the study, but could also have confounded

the interpretation and complicated comparison between groups, particularly if the number of experimental units and animals had not also been increased. This brings us to the already few experimental sites and animals in this study, which must be kept in mind when interpreting the study outcome. Another limitation of this study is the single and short healing time point of 6 weeks. Although studies have looked at the healing dynamics of similar bone defects grafted with DBBM at 8 weeks and beyond, little is still known about the temporal bone healing of defects grafted with WPTG. In order to answer this, further studies with multiple time points is required. The rationale for the short healing time in the present study was the hypothesis that the materials would differ in ability to support and stabilize the dental implants because of different mechanical properties, which did not require a longer healing time to assess. During installation, care was taken to ensure leveled implant placement. However, small apico-coronal, bucco-lingual or mesio-distal deviations may have had an impact on the analyses as the former defect compartment was defined from the implant shoulder. Thus, old bone may have been included in the areal histomorphometric analysis for a few sites, although only the most central section was used for this analysis. This impact is not limited to a specific group as the defects were made prior to application of the bone graft substitutes.

The two different particulate bone graft substitute materials demonstrated different mechanical properties, but the higher compressive strength and resistance to compact volume reduction observed for the WPTG granules seemed to be of negligible relevance for the early stability and osseointegration of implants, when grafted in marginal circumferential bone defects. The hypothesis was rejected as the results did

not indicate improved implant stability, osseointegration and osseous healing with the use of the mechanically stronger particulate bone graft substitute material.

### **Acknowledgements**

This study was in part sponsored by a grant from Tigran Technologies AB, Malmö, Sweden. Professor Lyngstadaas is a scientific advisor to the board of directors of Tigran Technologies AB. Professor Lyngstadaas and Dr. Wohlfahrt have received financial reimbursement when lecturing for Tigran Technologies AB.

## References

1. Botticelli D, Berglundh T, Lindhe J. Resolution of bone defects of varying dimension and configuration in the marginal portion of the peri-implant bone. An experimental study in the dog. *J Clin Periodontol* 2004; 31: 309–317
2. Ortega-Martínez J, Pérez-Pascual T, Mareque-Bueno S, Hernández-Alfaro F, Ferrés-Padró E. Immediate implants following tooth extraction. A systematic review. *Med Oral Patol Oral Cir Bucal* 2012; 17: e251–61
3. Esposito M, Grusovin MG, Polyzos IP, Felice P, Worthington HV. Interventions for replacing missing teeth: dental implants in fresh extraction sockets (immediate, immediate-delayed and delayed implants). *Cochrane Database Syst Rev* 2010: doi: 10.1002/14651858.CD005968.pub3
4. Shin SY, Shin SI, Kye SB, Chang SW, Hong J, Paeng JY, Yang SM. Bone cement grafting increases implant primary stability in circumferential cortical bone defects. *J Periodontal Implant Sci* 2015; 45: 30-35
5. Sabtrasekh R, Tiainen H, Lyngstadaas SP, Reseland J, Haugen HJ. A novel ultra-porous titanium dioxide ceramic with excellent biocompatibility. *J Biomater Appl* 2011; 25: 559-580
6. Wohlfahrt JC, Monjo M, Rønold HJ, Aass AM, Ellingsen JE, Lyngstadaas SP. Porous titanium granules promote bone healing and growth in rabbit tibia peri-implant osseous defects. *Clin Oral Implants Res* 2010; 21: 165–173
7. Verket A, Lyngstadaas SP, Rønold HJ, Wohlfahrt JC. Osseointegration of dental implants in extraction sockets preserved with porous titanium granules- an experimental study. *Clin Oral Implants Res* 2014; 25(2): e100-108

8. Polyzois I, Renvert S, Bosshardt DD, Lang NP, Claffey N. Effect of Bio-Oss on osseointegration of dental implants surrounded by circumferential bone defects of different dimensions: an experimental study in the dog. *Clin Oral Implants Res* 2007; 18: 304–310
9. Botticelli D, Berglundh T, Lindhe J. The influence of a biomaterial on the closure of a marginal hard tissue defect adjacent to implants. An experimental study in the dog. *Clin Oral Implants Res* 2004; 15: 285–292
10. Antunes AA, Oliveiro Neto P, de Santis E, Caneva M, Botticelli D, Salata LA. Comparisons between Bio-Oss(®) and Straumann(®) Bone Ceramic in immediate and staged implant placement in dogs mandible bone defects. *Clin Oral Implants Res* 2013; 24: 135-42
11. Butz F, Ogawa T, Chang TL, Nishimura I. Three-dimensional bone-implant integration profiling using micro-computed tomography. *Int J Oral Maxillofac Implants* 2006; 21: 687-695
12. Donath K, Breuner G. A method for the study of undecalcified bones and teeth with attached soft tissues. The Säge-Schliff (sawing and grinding) technique. *J Oral Pathol* 1982; 11: 318-326
13. Rohrer MD, Schubert CC. The cutting-grinding technique for histologic preparation of undecalcified bone and bone-anchored implants. Improvements in instrumentation and procedures. *Oral Surg Oral Med Oral Pathol* 1992; 74: 73-78
14. Misch CE, Qu Z, Bidez MW. Mechanical properties of trabecular bone in the human mandible: Implications for dental implant treatment planning and surgical placement. *J Oral Maxillofac Surg* 1999; 57: 700-706
15. Akimoto K, Becker W, Persson R, Baker DA, Rohrer MD, O'Neal RB. Evaluation of titanium implants placed into simulated extraction sockets: a study in dogs. *Int J Oral Maxillofac Implants* 1999 ; 14: 351-360
16. Stentz W, Mealey BL, Gunsolley JC, Waldrop TC. Effects of guided bone regeneration around commercially pure titanium and hydroxyapatite-coated dental implants. II. Histologic analysis. *J Periodontol* 1997; 68: 933-949
17. de Barros RRM, Novaes Jr AB, Queiroz A, Goncalves de Almeida AL. Early peri-implant endosseous healing of two implant surfaces placed in surgically created circumferential defects. A histomorphometric and fluorescence study in dogs. *Clin Oral Implants Res* 2012; 23: 1340-1351
18. Ito Y, Sato D, Yoneda S, Ito D, Kondo H, Kasugai S. Relevance of resonance frequency analysis to evaluate dental implant stability: simulation and histomorphometrical animal experiments. *Clin Oral Implants Res* 2008; 19: 9-14
19. Davies JE. Mechanisms of endosseous integration. *Int J Prosthodont* 1998; 11:

20. Botticelli D, Berglundh T, Buser D, Lindhe J. Appositional bone formation in marginal defects at implants. An experimental study in the dog. *Clin Oral Implants Res* 2003 : 14: 1-9
21. Rossi F, Botticelli D, Pantani F, Pereira FP, Salata LA, Lang NP. Bone healing pattern in surgically created circumferential defects around submerged implants: an experimental study in dog. *Clin Oral Implants Res* 2012: 23: 41–48
22. Chen ST, Wilson TG, Hämmerle CHF. Immediate or early placement of implants following tooth extraction: review of biologic basis, clinical procedures, and outcomes. *Int J Oral Maxillofac Implants* 2004 : 19 Suppl: 12–2
23. Guler B, Ahu U, Yalim M, Suleyman B. The comparison of porous titanium granule and xenograft in the surgical treatment of peri-implantitis: a prospective clinical study. *Clin Implant Dent Relat Res* 2016: doi: 10.1111/cid.12453

## Figure 1

- A) Implant placement after circumferential defect preparation prior to grafting.
- B) Suturing the implants and the grafted peri-implant defects prior to submerged healing.

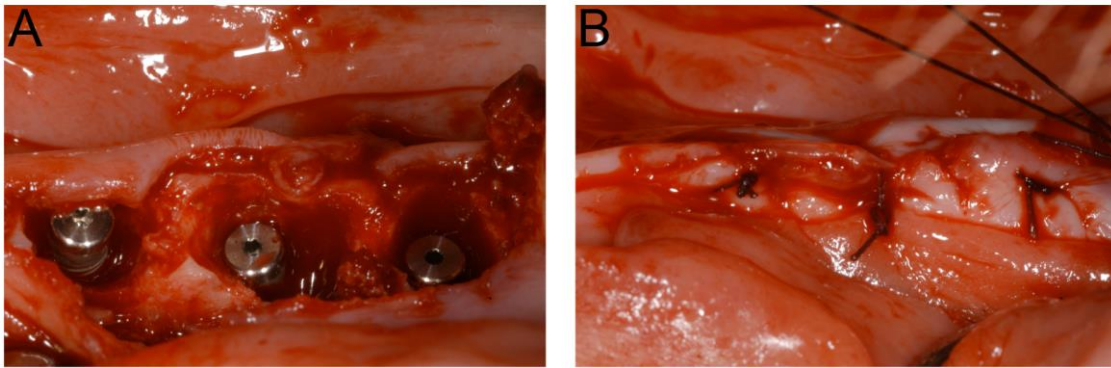


## Figure 2

(Left) Illustration of the volume of interest (VOI) analyzed by microcomputed tomography.

(Right) Image to illustrate the histomorphometric analysis. Image composed of multiple smaller microphotographs obtained at 25 X original magnification. Green frame = former defect area, Red area = Bone, Blue area = Graft material (DBBM), Pink arrows = First bone to implant contact (FBIC). The implant perimeter is labeled yellow if bone to implant contact, and blue if no bone to implant contact. The area within the former defect not designated a specific color consists of non-mineralized loose vascular connective tissue, soft tissue, bone marrow spaces or no cellular content.

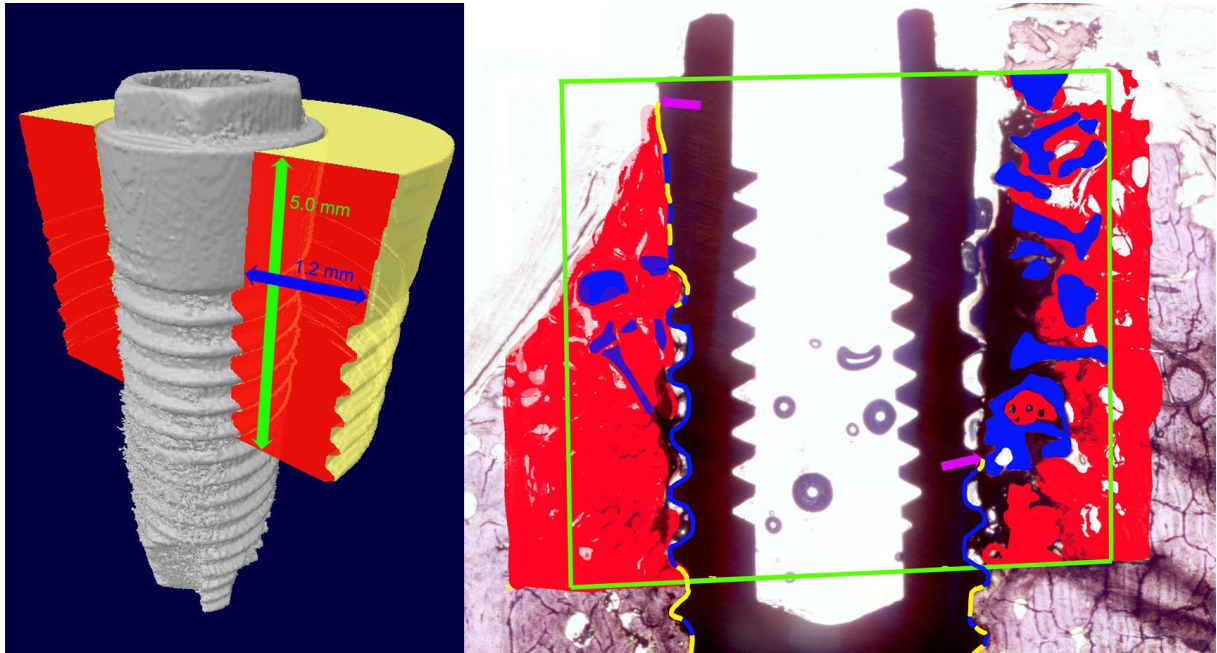


**Figure 3**

SEM images of PTG (left side), WPTG (middle) and DBBM (right side) at different magnifications. Different surface textures and porosity can be observed. The intragranular porosity is higher in the PTG and WPTG granules. In the higher magnifications, the structure appear rougher and more irregular on the surface of the WPTG and DBBM granules.

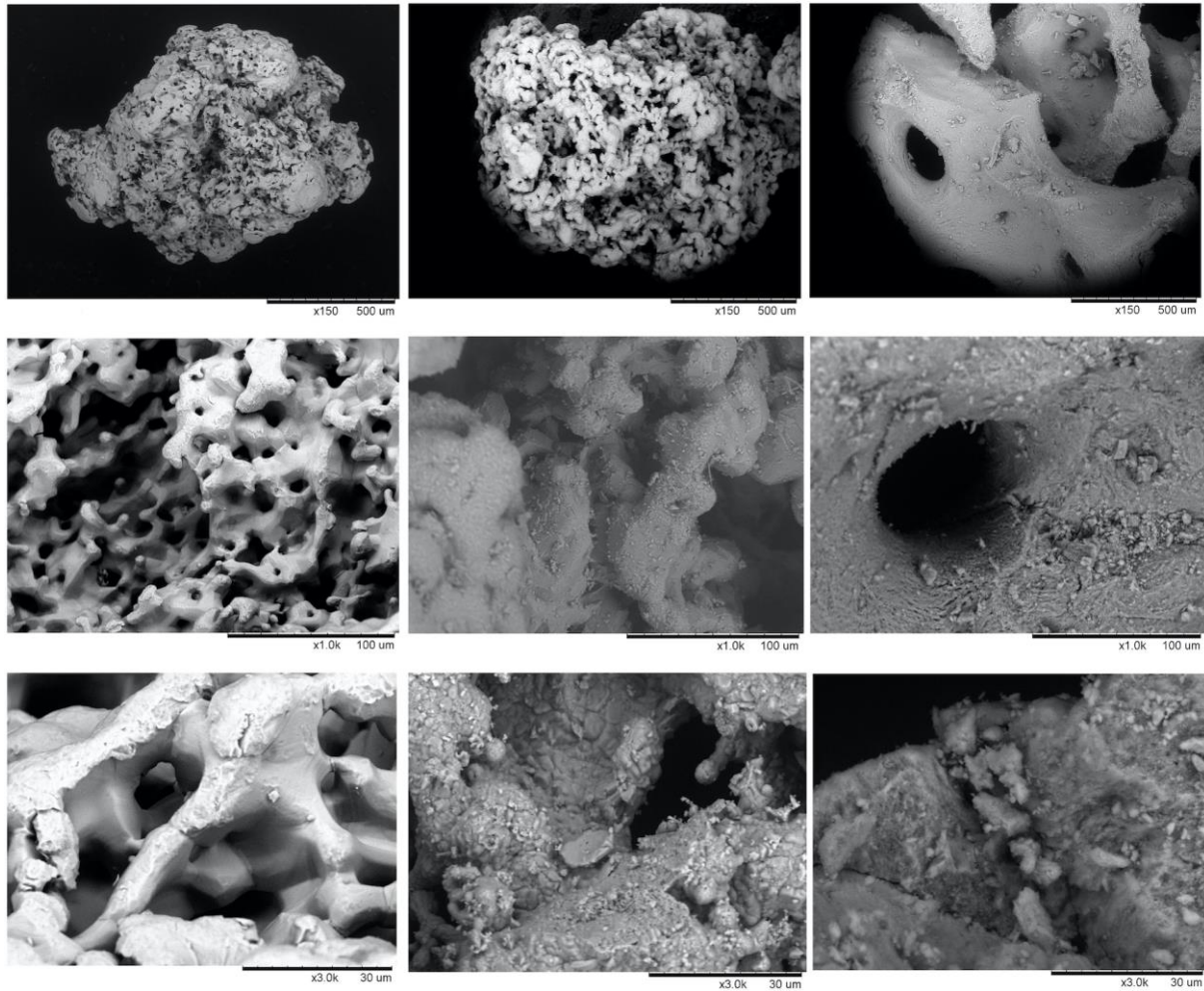


**Figure 4**

Top right: Bar graph demonstrating the mean compressive strength and standard deviation for each material. Top left: Bar graph demonstrating the mean compact volume reduction and standard deviation for each material. Lower right: Stress-strain curve for each material (n=3) Lower left: Curve displaying interconnectivity. WPTG: White porous titanium granules. DBBM: Demineralized bovine bone mineral. PTG: Porous titanium granules.

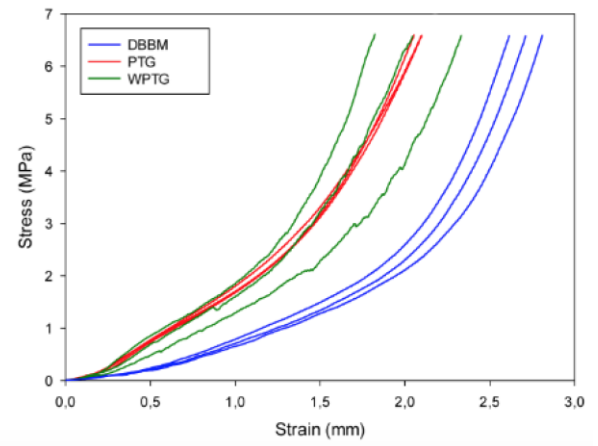
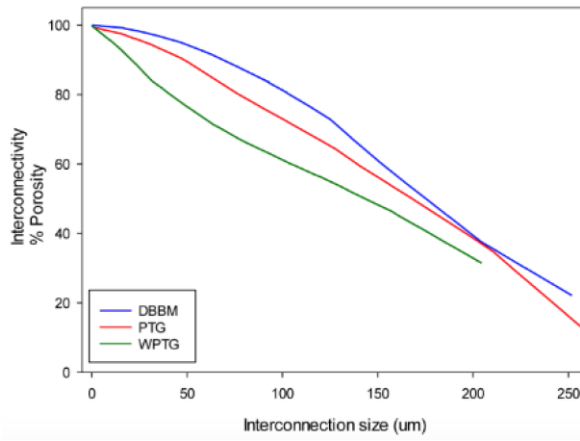
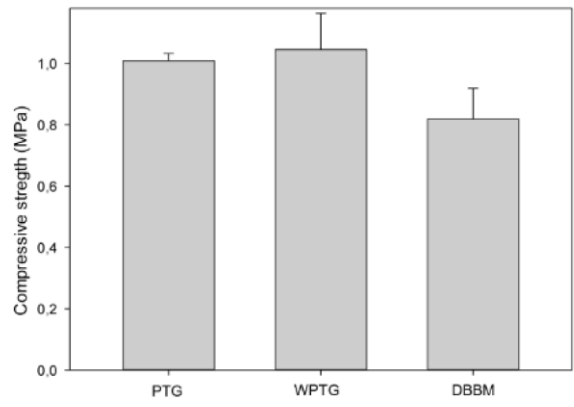
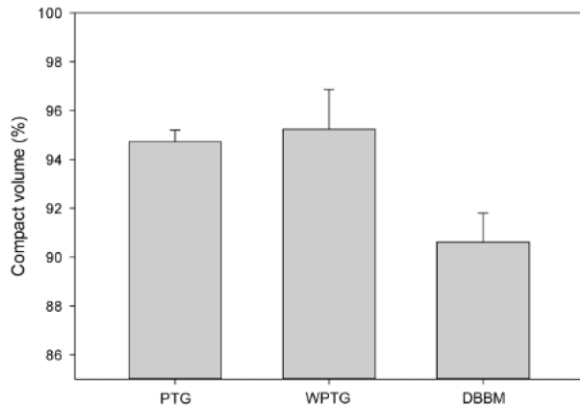


## Figure 5

Image composed of multiple smaller microphotographs obtained at 25 X original magnification. NB= New bone, WPTG= White porous titanium granules, LC= Non-mineralized loose vascular connective tissue, DBBM= Demineralized bovine bone mineral, Green line = Defect width demarcation.

**A)** Implant in WPTG group surrounded by new bone formation not invading the implant threads.

**B)** Sham site demonstrating pronounced new bone formation not invading the implant threads.

**C)** WPTG site demonstrating graft particles embedded both in new bone and in non-mineralized loose vascular connective tissue.

**D)** DBBM site demonstrating graft particles embedded both in new bone and in non-mineralized loose vascular connective tissue.

**E)** Newly formed bone is scarce at the base of the defect, but is evident in the more coronal part of the defect. DBBM particles can be observed throughout the newly formed bone in the former defect.

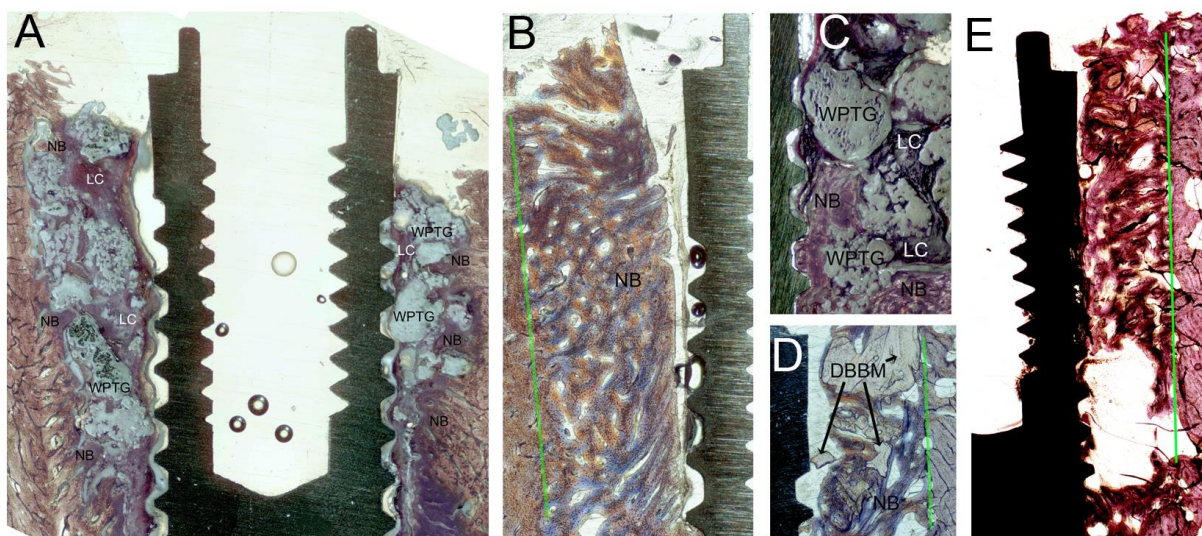


**Figure 6**

Column graph illustrating the bone-to-implant contact (%) (left), defect bone fill (%) (middle) and the distance of first bone-to-implant contact (mm) measured from the implant neck (right).

